Journal of Magnetic Resonance 205 (2010) 235–241

Contents lists available at ScienceDirect

Journal of Magnetic Resonance

journal homepage: www.elsevier.com/locate/jmr

Simplified and scalable numerical solution for describing multi-pool chemical exchange saturation transfer (CEST) MRI contrast

Phillip Zhe Sun *

Athinoula A. Martinos Center for Biomedical Imaging, Department of Radiology, Massachusetts General Hospital and Harvard Medical School, Charlestown, MA 02129, United States

ARTICLE INFO

Article history:
Received 2 February 2010
Revised 6 May 2010
Available online 10 May 2010

Keywords:
Amide proton transfer (APT)
Chemical exchange saturation transfer (CEST)
Numerical solution

ABSTRACT

Chemical exchange saturation transfer (CEST) imaging is sensitive to dilute labile proton and microenvironment properties such as pH and temperature, and provides vital information complementary to the conventional MRI methods. Whereas the Bloch equations coupled by exchange terms (i.e., Bloch–McConnell equations) have been utilized to quantify 2-pool CEST contrast, it is tedious to extend the Bloch–McConnell equations to describe CEST contrast beyond four saturation transfer sites. Hence, it is necessary to develop a scalable yet reasonably accurate numerical solution to describe the complex multi-pool CEST contrast. It is postulated here that the multi-pool CEST contrast can be quantified by modifying the classic 2-pool model. Although the direct exchange among labile proton groups is often negligible, labile protons may be coupled indirectly through their interaction with bulk water protons, which has to be quantified. The coupling term was solved empirically, and the proposed simplified solution was shown in good agreement with the conventional simulation. Moreover, the proposed solution is scalable, and can be easily extended to describe multi-pool CEST contrast. In sum, our study established a simplified and scalable, yet reasonably accurate numerical solution, suitable for quantitatively describing multi-pool CEST contrast.

1. Introduction

The indirect detection mechanism of chemical exchange saturation transfer (CEST) MRI confers it with an enormous sensitivity enhancement so that dilute labile proton and microenvironment properties such as pH and temperature can be estimated [1,2]. Specifically, CEST contrast is approximately proportional to the labile proton concentration and exchange rate, hence, provides information that complements the conventional imaging methods [3–6]. For instance, CEST MRI is capable of measuring metabolites and their byproducts such as glucose, glycogen and lactate [7–9]. In addition, amide proton transfer (APT) imaging, a specific form of CEST MRI, is pH dependent and remains promising for detecting ischemic tissue acidosis beyond the commonly used perfusion and diffusion scans [10–14]. Nevertheless, CEST MRI contrast is complex; it not only varies with labile proton concentration, exchange rate and relaxation time, but also depends on the experimental parameters such as the magnetic field strength, RF power, duration and scheme [15–19]. In addition, when there are multiple exchangeable proton groups within a single CEST system, quantitative description of CEST contrast becomes even more complex [13,20–23]. Moreover, semisolid macromolecular magnetization transfer (MT) and nuclear overhauser effect (NOE)-mediated saturation transfer may also become non-negligible for *in vivo* CEST MRI, particularly so if large RF irradiation power is applied [22,24–27].

Mathematical models have been developed to describe CEST contrast [27–31]. Specifically, an empirical solution based on the 2-pool exchange model provides simple yet reasonably accurate quantification of CEST contrast [15,19]. The solution has also been modified to describe *in vivo* pH-weighted APT imaging of acute ischemia [31]. While on the other hand, Bloch equations coupled with exchange terms (Bloch–McConnell equations) can also numerically simulate 2-pool chemical exchange, and has been recently extended for quantifying 3-pool and 4-pool CEST contrast [27,30]. However, conventional Bloch–McConnell equations are not easily scalable, and it is somewhat tedious to apply it to describe multi-pool CEST contrast beyond three labile proton groups. While on the other hand, over ten saturation transfer sites have been identified in biological systems, and therefore, it is necessary to develop a simplified solution for describing complex multi-pool CEST contrast [13,22,23,32].

To address this need, our study investigated whether the multi-pool CEST contrast can be simulated using the commonly used 2-pool exchange model. It is important to note that because the direct RF saturation should be taken into account only once, multi-pool CEST Z-spectrum cannot be obtained by simply superimposing

* Address: Rm 2301, 149 13th Street, Athinoula A. Martinos Center for Biomedical Imaging, Department of Radiology, Massachusetts General Hospital, Harvard Medical School, Charlestown, MA 02129, United States. Fax: +1 617 726 7422.
E-mail address: pzhesun@nmr.mgh.harvard.edu

1090-7807/$ - see front matter © 2010 Elsevier Inc. All rights reserved.
doi:10.1016/j.jmr.2010.05.004

multiple Z-spectra estimated independently. Fortunately, the direct RF saturation can be quantified using a single set of Bloch equations [30,33]. In addition, whereas direct exchange among labile proton groups is negligible due to their dilute concentration, labile protons may be coupled indirectly through their saturation transfer with bulk water protons. Particularly, when the RF irradiation amplitude becomes comparable with their chemical shifts, multiple labile protons may be simultaneously saturated, thus, compete for CEST contrast. As a result, simple linear superposition of individual CEST contrast will overestimate the multi-pool CEST contrast. Our study here derived the coupling term and developed a simplified solution, based on the classic 2-pool model, to quantify multi-pool CEST MRI contrast. We first confirmed that the proposed method is in good agreement with the conventional multi-pool CEST simulation using a representative 3-pool CEST system. We then showed that the proposed method is scalable and can be easily extended to simulate multi-pool CEST contrast with only minimal modification. In summary, the proposed numerical solution method provides simplified yet reasonably accurate modeling of multi-pool CEST contrast, suitable for quantifying complex CEST contrast.

2. Theory

Bloch–McConnell equations are often used to describe CEST contrast, and for a representative 2-pool chemical exchange, we have [28,30],

$$\begin{bmatrix} \partial M_{wx}/\partial t \\ \partial M_{wy}/\partial t \\ \partial M_{wz}/\partial t \\ \partial M_{sx}/\partial t \\ \partial M_{sy}/\partial t \\ \partial M_{sz}/\partial t \end{bmatrix} = \begin{bmatrix} -k_{ws} & \Delta\omega_w & 0 & k_{sw} & 0 & 0 \\ \Delta\omega_w & -k_{ws} & -\omega_1 & 0 & k_{sw} & 0 \\ 0 & -\omega_1 & -k_{ws} & 0 & 0 & k_{sw} \\ k_{ws} & 0 & 0 & -k_{sw} & \Delta\omega_s & 0 \\ 0 & k_{ws} & 0 & \Delta\omega_s & -k_{sw} & -\omega_1 \\ 0 & 0 & k_{ws} & 0 & -\omega_1 & -k_{sw} \end{bmatrix} \begin{bmatrix} M_{wx} \\ M_{wy} \\ M_{wz} \\ M_{sx} \\ M_{sy} \\ M_{sz} \end{bmatrix} - \begin{bmatrix} M_{wx}/T_{2w} \\ M_{wy}/T_{2w} \\ (M_{w0}-M_{wz})/T_{1w} \\ M_{sx}/T_{2s} \\ M_{sy}/T_{2s} \\ (M_{s0}-M_{sz})/T_{1s} \end{bmatrix} \tag{1}$$

in which $M_{wx,y,z}$ and $M_{sx,y,z}$ are the x, y and z magnetization components for bulk water and labile protons, respectively, with $T_{1,2w}$ and $T_{1,2s}$ being their longitudinal and transverse relaxation time. In addition, k_{sw} and k_{ws} are chemical exchange rate from labile group to bulk water and vise versa. Moreover, ω_1 is the RF irradiation amplitude, and $\Delta\omega_{w,s}$ is the difference between irradiation RF offset and the bulk water and labile proton chemical shifts, respectively. Because the transverse relaxation rate of labile protons may not be negligible when compared with the exchange rate, the transverse magnetization exchange is also included. The Bloch–McConnell equation can be extended to describe multi-pool CEST contrast as [30]

While very useful, such a solution is not flexible and may not be easily extended to describe complex multi-pool CEST contrast, beyond four saturation transfer sites.

To address this, the current study aims to develop a simplified numerical solution to simulate multi-pool CEST contrast. Specifically, the magnetization transfer ratio (MTR) is defined as,

$$\mathrm{MTR}(\omega_1,\Delta\omega) = 1 - I(\omega_1,\Delta\omega)/I_0 \tag{3}$$

in which I and I_0 are the MR signal with and without RF pre-saturation, and ω_1 and $\Delta\omega$ are the RF irradiation amplitude and offset, respectively. For a simplistic 2-pool model, MTR is a function of RF offset (Z-spectrum) with two prominent attenuations around the labile proton ($\Delta\omega_s$) and bulk water ($\Delta\omega_w$) chemical shifts. For dilute labile protons undergoing slow or intermediate chemical exchange, CEST contrast can be obtained by removing the direct RF saturation effect from Z-spectrum as,

$$\mathrm{CESTR}(\omega_1,\Delta\omega_s) = \mathrm{MTR}(\omega_1,\Delta\omega) - \mathrm{MTR}(\omega_1,\Delta\omega_w) \tag{4}$$

where MTR (ω_1, $\Delta\omega_w$) is the direct RF saturation effect, which can be derived either by the analytical solution or the classical Bloch equation [30,33]. For multiple well-separated CEST groups, the first order approximation of CEST contrast may be obtained by superimposing CEST contrasts of each labile proton independently as

$$\mathrm{CESTR}(\omega_1,\Delta\omega) = \sum_i \mathrm{CESTR}_i(\omega_1,\Delta\omega_{si}) \tag{5}$$

where $\Delta\omega_{si}$ is the chemical shift offset of the ith labile group. It is important to note that although the direct exchange among labile protons is often negligible, they may interact indirectly via bulk water signals. Hence, the coupling term has to be derived in order to extend the classical 2-pool model to describe multi-pool CEST contrast. We solved the coupling term (see Appendix A) and the multi-pool CEST MRI contrast can be shown to be,

$$\begin{aligned}\mathrm{CESTR}(\omega_1,\Delta\omega) \approx{}& \sum_i \mathrm{CESTR}_i(\omega_1,\Delta\omega_{si}) \\ &- \sum_{i>j} \begin{bmatrix} \mathrm{CESTR}_i(\omega_1,\Delta\omega_{si}) * \mathrm{CESTR}_j(\omega_1,\Delta\omega_{sj}) * \\ (2 - \mathrm{CESTR}_i(\omega_1,\Delta\omega_{si}) - \mathrm{CESTR}_j(\omega_1,\Delta\omega_{sj})) \end{bmatrix}\end{aligned} \tag{6}$$

$$\begin{bmatrix} \partial M_{wx}/\partial t \\ \partial M_{wy}/\partial t \\ \partial M_{wz}/\partial t \\ . \\ . \\ . \\ \partial M_{s_{n-1}x}/\partial t \\ \partial M_{s_{n-1}y}/\partial t \\ \partial M_{s_{n-1}z}/\partial t \end{bmatrix} = \begin{bmatrix} -k_{ws_1} & \Delta\omega_w & 0 & . & 0 & 0 & k_{s_{n-1}w} & 0 & 0 \\ \Delta\omega_w & -k_{ws_1} & -\omega_1 & 0 & . & 0 & 0 & k_{s_{n-1}w} & 0 \\ 0 & -\omega_1 & -k_{ws_1} & 0 & 0 & . & 0 & 0 & k_{s_{n-1}w} \\ . & . & 0 & 0 & . & . & 0 & 0 & 0 \\ . & 0 & . & 0 & . & . & -\omega_1 & 0 & 0 \\ . & 0 & 0 & . & 0 & -\omega_1 & . & 0 & 0 \\ k_{ws_{n-1}} & 0 & 0 & 0 & 0 & 0 & -k_{s_{n-1}w} & \Delta\omega_{s_{n-1}} & 0 \\ 0 & k_{ws_{n-1}} & 0 & 0 & 0 & 0 & \Delta\omega_{s_{n-1}} & -k_{s_{n-1}w} & -\omega_1 \\ 0 & 0 & k_{ws_{n-1}} & 0 & 0 & 0 & 0 & -\omega_1 & -k_{s_{n-1}w} \end{bmatrix} \begin{bmatrix} M_{wx} \\ M_{wy} \\ M_{wz} \\ . \\ . \\ . \\ M_{s_{n-1}x} \\ M_{s_{n-1}y} \\ M_{s_{n-1}z} \end{bmatrix} - \begin{bmatrix} M_{wx}/T_{2w} \\ M_{wy}/T_{2w} \\ (M_{w0}-M_{wz})/T_{1w} \\ . \\ . \\ . \\ M_{s_{n-1}x}/T_{2s_{n-1}} \\ M_{s_{n-1}y}/T_{2s_{n-1}} \\ (M_{s_{n-1}0}-M_{s_{n-1}z})/T_{1s_{n-1}} \end{bmatrix} \tag{2}$$

3. Materials and methods

Numerical simulation was conducted in Matlab 7.4 (Mathworks, Natick MA). The coupling term was first derived, and the proposed simplified solution was compared with the conventional numerical solution using a representative 3-pool CEST model. We assumed that the T_1 and T_2 for bulk water are 3 s and 100 ms, respectively, and being 1 s and 15 ms for two dilute labile protons. In addition, the chemical shifts for two labile protons were set to be 4 and 5 ppm, for the magnetic field strength of 4.7 T (200 MHz). Moreover, we serially varied the labile proton concentration and exchange rate, and evaluated the proposed solution for a representative 3-pool CEST model. Furthermore, we examined the effects of RF amplitude and chemical shift. Specifically,

(1) *Labile proton concentration*: We varied both labile proton concentration from 1:2000 to 1:500, with respect to the bulk water protons, and their exchange rates were assumed to be 100 and 300 s^{-1} for chemical shifts of 4 and 5 ppm, respectively, and B_1 = 1 μT (43 Hz).
(2) *Chemical exchange rate*: We examined slow and intermediate chemical exchange, from 10 to 200 s^{-1}, for both labile proton groups. Their concentrations were assumed to be 1:500 and 1:1000 for chemical shifts of 4 and 5 ppm, respectively, and B_1 = 1 μT.
(3) *RF irradiation amplitude*: We varied the RF irradiation amplitude from 0.1 to 2 μT, and reexamined the proposed method. Aforementioned labile proton concentration, exchange and relaxation rates, chemical shift offset and field strength were assumed.
(4) *Chemical shift*: We also investigated the chemical shift dependence of the proposed numerical solution, particularly, in the presence of sizeable overlap of CEST spectra. We maintained the chemical shift for one labile group at 5 ppm, and systematically varied the chemical shift for the second group from 4 to 6 ppm. Similar labile proton concentration, exchange and relaxation rates, RF amplitude and field strength were assumed. It is also important to note that the simulated exchange rate and chemical shift are typical values for diamagnetic CEST agents, and hence, our conclusions may not necessarily be applicable for paramagnetic CEST (PARACEST) agents, as their exchange rate, chemical shift and local concentration as well as experimental parameters are drastically different from those simulated here.

Finally, we demonstrated the scalability of the propose solution by simulating the CEST contrast of five dilute saturation transfer sites, which conventionally takes a 6-pool exchange model to describe. Specifically, we simulated one amide group, two hydroxyl groups and two nuclear overhauser effect (NOE) sites [9,13,22,23,32]. Their chemical shifts, with respect to the water resonance, were 3.65, 2.3, 1.2, −3 and −3.5 ppm, respectively. In addition, their labile proton concentrations were set to be 1:1000, 1:1000, 1:500, 1:500 and 1:500, while their exchange rates set to be 50, 50, 50, 10 and 10 s^{-1}, respectively. Moreover, T_1 for all labile protons was assumed to be 1 s, which should only minimally affect the simulated CEST contrast due to that only steady state was solved, while their T_2 was chosen to be 15, 5, 10, 5 and 5 ms, respectively. In addition, two representative RF amplitudes of 1 and 2 μT were simulated. It is necessary to note that the exchange rate and relaxation rates for the NOE sites were assumed to be similar as those of diamagnetic CEST agents, simply to illustrate the scalability of the proposed solution [13,32]. Their exact values for a given specific system, once derived, can be easily incorporated to the numerical solution.

4. Results

Fig. 1 compares the proposed scalable solution with the conventional simulation of multi-pool CEST contrast. The conventional simulation (Fig. 1a) utilizes multiple sets of Bloch equations coupled by the exchange terms, with each set representing a single labile proton group [28]. The Bloch matrix size, for a general N-saturation transfer sites, is 3 N by 3 N ($O(N^2)$). In comparison, the proposed simplified solution utilizes multiple 2-pool models, with a correction term that takes into account of the indirect coupling effect (Fig. 1b). As such, it includes (N–1) sets of 2-pool exchangeable models (O(N)), significantly reduced from that of the conventional approach when N becomes large.

We evaluated the proposed simplified solution using a representative 3-pool CEST system, i.e., two 2-pool solution vs. a conventional 3-pool solution. The two labile protons were assumed to be at 4 and 5 ppm, and their concentrations were assumed to be 1:250 and 1:500, with exchange rates of 100 s^{-1} and 300 s^{-1}, respectively (Fig. 2a). Moreover, T_1 and T_2 for bulk water were assumed to be 3 s and 100 ms, being 1 s and 15 ms for both labile protons. In addition, we set the magnetic field strength to be 4.7 T, and solved the CEST contrast for a long (7.5 s) continuous wave (CW) RF irradiation field of 1 μT. Z-spectra for the two labile protons were simulated independently using the 2-pool model (Fig. 2b). Fig. 2c shows the CEST contrast for 4 and 5 ppm, in black and gray, respectively, obtained by subtracting the direct RF saturation contribution from the two Z-spectra. In addition, the linear superposition of two CEST spectra was shown in light gray dash dotted line, while the proposed simplified solution is shown in a dotted line, slightly less than the simplistic linear superposition. Fig. 2d compared the Z-spectra obtained by the simplistic linear superposition (gray, Eq. (5)), the proposed simplified solution (dotted, Eq. (6)) and the conventional 3-pool simulation solution (gray dash dotted). While the simplistic linear superposition solution differed from conventional simulation by 7%, the maximal difference between the proposed solution and the conventional simulation is less than 0.2%. As such, we showed that the proposed solution, by including the coupling term, agreed very well with conventional Bloch–McConnell solution.

We also evaluated the precision of the proposed simplified numerical solution by comparing it with the conventional 3-pool

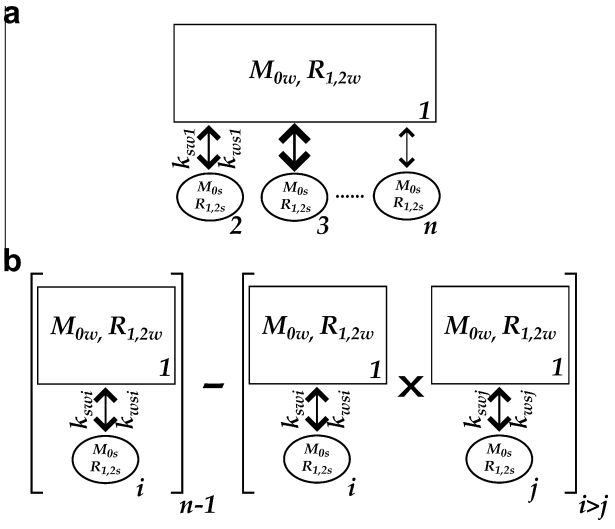

Fig. 1. (a) The conventional modeling of multi-pool CEST contrast was based on the Bloch–McConnell equations, with each saturation transfer site represented by a set of Bloch equations. (b) The proposed simplified solution describes the multi-pool CEST contrast by modifying multiple sets of 2-pool exchange models, with a correction term to take into account of the coupling among CEST contrasts.

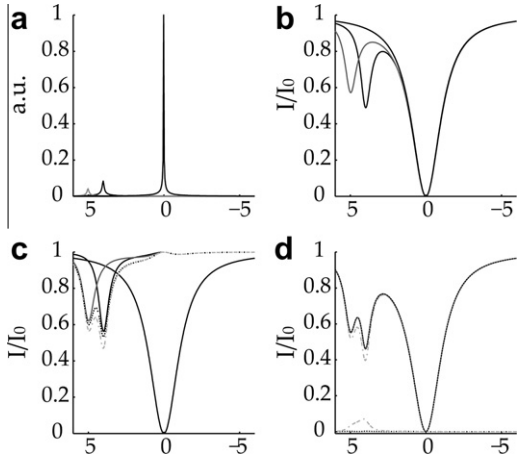

Fig. 2. Comparison of the proposed simplified solution with the conventional simulation using a representative 3-pool mode: bulk water and two dilute labile groups at 4 and 5 ppm. (a) Simulated spectrum showing the dilute labile proton (magnified by 100) and bulk water peaks. (b) Z-spectra for each labile group simulated independently using the classic 2-pool model, as well as the direct RF saturation effect. (c) CEST contrast estimated by subtracting direct RF saturation effect from Z-spectra, which showed two prominent CEST peaks at 4 and 5 ppm in black and gray, respectively. In addition, the simplistic linear superposition of CEST contrasts and the proposed simplified solution were shown in gray dash dotted and dotted lines, respectively. (d) Whereas the simplistic linear superposition (gray dash dotted) differed from the conventional 3-pool simulation (black line) by 7%, the proposed solution (dotted) agreed very well and in fact, overlapped with the conventional solution, within 0.2%.

model for a typical range of labile proton concentration and exchange rate (Fig. 3). When the labile proton concentration for both exchangeable groups was increased from 1:2000 to 1:500, the CESTR, calculated as the MTR asymmetry at 4 and 5 ppm, increased almost linearly with the concentration (Fig. 3a). In fact, the CESTR obtained from both solutions nearly overlapped, and their maximal difference is less than 0.2% (Fig. 3b). In addition, CESTR also increased with exchange rate (Fig. 3c). It is noticeable that the slope of CESTR increment with respect to exchange rate decreased at high exchange rates, likely because the saturation efficiency is reduced when the CEST contrast competes with the T_1 relaxation (Fig. 3c). The two solutions agreed very well, with their maximal difference being less than 0.1% (Fig. 3d).

Our study also evaluated the proposed solution while varying the RF amplitude and chemical shift (Fig. 4). Fig. 4a shows that the CESTR initially increased with RF amplitude, peaking at approximately 1 μT for labile protons at 4 ppm, and 2 μT for labile protons at 5 ppm (Fig. 4a). In fact, the two solutions agreed reasonably well, with their maximal difference less than 1% (Fig. 4b). Moreover, when the chemical shift of one labile proton was varied from 4 to 6 ppm, while the other group remained at 5 ppm, the proposed solution also agreed well with the conventional simulation (Fig. 4c). Because the CEST contrast was derived as the MTR asymmetry at their individual chemical shift, the calculated CESTR is susceptible to the coupling term of two CEST groups. This was particularly the case when the chemical shift of the second pool was 5 ppm, overlapping with that of the first pool (Fig. 4c). Nevertheless, our proposed method agreed very well with the conventional 3-pool simulation, within 0.3% (Fig. 4d). Hence, our results showed that the proposed solution provides simplified yet reasonably accurate modeling of multi-pool CEST contrast.

To demonstrate the scalability of the proposed numerical solution, we simulated CEST contrast for an illustrative five saturation transfer sites, equivalent to the conventional 6-pool CEST model (Fig. 5). The hypothetical CEST system includes an exchangeable amide proton pools (3.65 ppm) and two hydroxyl protons (2.3 and 1.2 ppm) [9,13]. In addition, two aliphatic groups (−3 and −3.5 ppm) were added to model saturation transfer via NOE [22,23,32]. We also simulated two typical RF amplitudes of 1 and 2 μT. Fig. 5a shows that at low RF amplitude, the individual CEST contrast can be reasonably distinguished, while the frequency resolution of the Z-spectrum degraded at stronger RF amplitude due to the direct RF saturation effect and the coupling term among multiple saturation transfer sites [15,31]. The direct RF saturation effect was also simulated, shown in dotted and dash dotted lines in Fig. 5a. It is important to point out that very little modification was required when we extended the proposed solution from 3-pool to 6-pool, simply providing the inputs of the labile proton

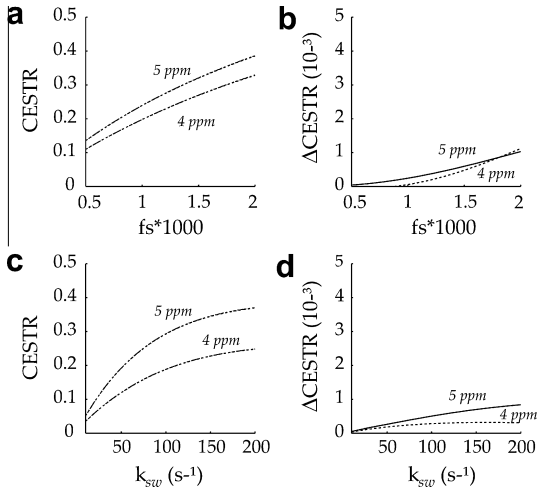

Fig. 3. Evaluation of the proposed solution as a function of labile proton concentration and exchange rate. (a) The labile proton concentration for both groups was varied from 1:2000 to 1:500, with their exchange rates assumed to be 100 and 300 s^{-1} for 4 and 5 ppm, respectively. The CEST contrast increased about linearly with labile proton concentration. (b) Simulation with both methods nearly overlapped, with their maximal difference less than 0.2%. (c) The CEST contrast increased with exchange rate when it was varied from 10 to 200 s^{-1}. (d) The simulation from both methods agreed very well, with the maximal difference less than 0.1%.

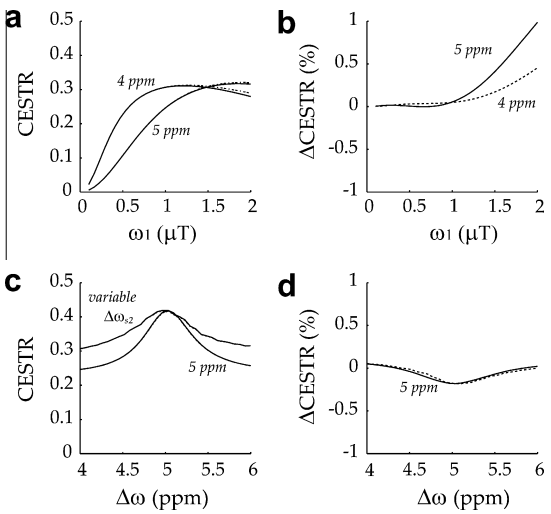

Fig. 4. Evaluation of the proposed solution as a function of RF amplitude and offset. (a) The CEST contrast initially increased with RF amplitude, but peaked and then subsequently decreased with higher RF amplitude. (b) Simulation from both methods agreed reasonably well, with the maximal difference less than 1%. (c) Simulated CEST contrast as a function of labile proton chemical shift. The chemical shift of one labile proton was set at 5 ppm, while the second labile group was serially varied from 4 to 6 ppm, at RF power level of 1 μT. (d) Two solutions nearly overlapped, with the maximal difference less than 0.2%.

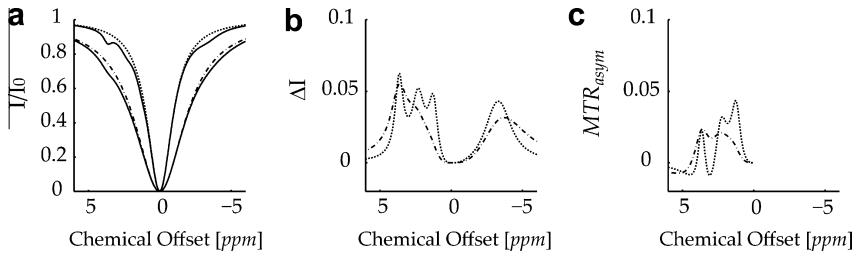

Fig. 5. Simulation of CEST contrast of five saturation transfer sites, being at 3.65, 2.3, 1.2, −3 and −3.5 ppm. The concentration of each site was assumed to be 1:1000, 1:1000, 1:500, 1:500 and 1:500, with their exchange rates being 50, 50, 50, 10 and 10 s^{-1}, respectively. (a) The simulated Z-spectra and direct RF saturation effect for RF amplitude of 1 and 2 μT was shown in dotted and dash dotted line, respectively. (b) The CEST contrast wa obtained by subtracting Z-spectra from RF spillover effects for two RF amplitudes. The frequency resolution of CEST contrast degraded with RF amplitude due to direct RF saturation effect and the coupling among CEST contrasts. (c) The RF amplitude-dependent MTR_{asym} may be significantly lower than the CEST contrast due to a negative shift attributable to NOE effects.

concentration, chemical shift, exchange and relaxation rates, without modification of the subroutines. Fig. 5b shows the CEST-specific contrast, as determined by subtracting each Z-spectrum from the corresponding direct RF saturation effect. At 1 μT, the CEST contrast of the –NH and –OH groups can be reasonably resolved, whereas two NOE sites showed significant overlap due to their relatively short T_2 and small chemical shift difference (Fig. 5b). Moreover, the MTR asymmetry (MTR_{asym}) was calculated by taking the difference between downfield and highfield MTR symmetrically around the bulk water signal (Fig. 5c). It showed that the CEST contrast may be underestimated unless the negative shift induced by saturation transfer effect from highfield offset (NOE effects) can be properly taken into account.

5. Discussion

This study developed a simplified numerical solution for describing multi-pool CEST contrast. The proposed method is scalable, and can be easily extended to describe CEST imaging of a large number of labile protons, potentially useful for quantifying *in vivo* CEST applications [13,22]. Whereas for the representative 3-pool CEST contrast, the computation time of the proposed method is comparable with that of conventional solution (~0.2 s, Dell Dimension 9100), the advantage in computation time and memory usage of the proposed solution may be realized when the number of CEST sites becomes large. It is so because whereas the Bloch matrix increase as the square of the number of saturation transfer site for the conventional simulation ($O(N^2)$), it increases only linearly for proposed solution ($O(N)$) [18,34]. In addition, the proposed method can be easily extended to simulate CEST contrast of large number of exchangeable proton groups without modification of subroutines, while the simulation codes for the conventional solution have to be rewritten each time the number of saturation transfer sites is varied. As such, the proposed solution is flexible and scalable, and if combined with water exchange spectroscopy (WEX) results, may significantly augment the quantitative CEST MRI, understanding which is vital for endogenous *in vivo* CEST imaging [13,22].

Our results suggested that when compared with Z-spectrum, the MTR asymmetry analysis may not be able to delineate CEST contrast from those related to saturation transfer due to high field offsets, often attributable to NOE/MT [22,25,35]. In fact, it has been shown that pH-weighted amide proton transfer (APT) imaging is susceptible to an intrinsic MT asymmetry shift (MTR'_{asym}) likely attributable to NOE [13,35]. Hence, whereas MTR asymmetry analysis provides fast estimation of CEST/APT-weighted contrast, additional insights can be gained by acquiring and analyzing the Z-spectra. It is also necessary to point out that the proposed numerical solution is based on Bloch equations, and as such, may be somewhat oversimplified for describing *in vivo* CEST contrast. It is so because the lorentzian spectral lineshape implicitly prescribed by the Bloch equation may deviate from that of semisolid macromolecules, which may be better represented by Gaussian or super-lorentzian functions. This problem is addressable, however, as several studies have shown that customized lineshape can be directly incorporated into the modified Bloch equations [27,36,37]. While on the other hand, MT contrast during *in vivo* CEST MRI may not be severe if RF amplitude is not too large. It is also important to bear in mind that because the concentration, chemical shift and exchange rate of paramagnetic CEST (PARACEST) agents as well as the commonly used RF amplitude are very different from those investigated in our study, the proposed simplified solution has to be reevaluated before it can be used to quantify PARACEST MRI contrast.

Finally, whereas the proposed solution is relatively flexible and can be extended to describe CEST imaging of essentially unlimited magnetization transfer sites, extra care is needed when the proposed solution is applied to derive exchange rates and concentrations of multiple saturation transfer sites from experimental measurements due to its multi-parametric non-linear nature. Because the proposed method may partition the fitting into multiple sets of 2-pool fittings and their coupling terms, the susceptibility to multi-parameter non-linear fitting errors for the proposed and conventional solutions may be slightly different. In addition, our results (Fig. 5) indeed suggested that by concurrently fitting multiple Z-spectra obtained with a reasonably spread of RF amplitudes, the precision and reliability of quantitative CEST contrast analysis may be improved [16,19,31]. Consequently, further study is needed to systematically evaluate the usefulness of the new solution for numerical fitting of CEST MRI results (simulated or experimentally obtained data), the reverse problem of the currently evaluated numerical simulation application.

6. Conclusion

A flexible numerical solution based on the classic 2-pool exchange model was developed to describe multi-pool CEST contrast, in good agreement with the conventional numerical simulation method. The proposed method is scalable and can be easily extended to describe CEST contrast of a large number of saturation transfer sites. As such, our work may facilitate quantitative understanding of complex CEST contrast, complementing the conventional numerical simulation methods.

Acknowledgments

This study was supported in part by Grants from AHA/SDG 0835384N, NIH/NIBIB 1K01EB009771-01 and NIH/R21NS061119-02.

Appendix A

To evaluate the proposed simplified solution, we partitioned a single group of labile protons into two groups, with identical chemical shift and exchange rate. We have $f = f_1 + f_2$, with f, f_1 and f_2 being the labile proton concentration for the complete pool and two partitioned pools, respectively. The CEST contrast of the complete labile proton can be shown to be [15]

$$\mathrm{CESTR} = \frac{f \cdot k_{sw}}{R_{1w} + f \cdot k_{sw}} \cdot \alpha \cdot (1 - \sigma) \tag{A.1}$$

where k_{sw} is the chemical exchange rate, α is labeling coefficient and σ is the spillover factor, while R_{1w} is the bulk water longitudinal relaxation rate. The labile proton concentration can be solved from Eq. (A.1), being

$$f = \frac{R_{1w}}{k_{sw}} \frac{\mathrm{CESTR}}{\alpha \cdot (1 - \sigma) - \mathrm{CESTR}} \tag{A.2}$$

For dilute labile protons undergoing slow or intermediate chemical exchange, it can be shown that the labeling coefficient and spillover factor have very little dependence upon labile proton concentration. In addition, such effects have already been taken into account when the Z-spectrum is simulated, and hence, the labile proton concentration can be approximated by $f \approx \frac{R_{1w}}{k_{sw}} \cdot \frac{\mathrm{CESTR}}{1-\mathrm{CESTR}}$. The same relationship also applies to the partitioned labile proton concentration, namely, $f_i \approx \frac{R_{1w}}{k_{sw}} \cdot \frac{\mathrm{CESTR}_i}{1-\mathrm{CESTR}_i}$, with $i = 1$ and 2.

The relationship of $f = f_1 + f_2$ can now be rewritten as

$$\begin{aligned} \frac{\mathrm{CESTR}}{1-\mathrm{CESTR}} &= \frac{\mathrm{CESTR}_1}{1-\mathrm{CESTR}_1} + \frac{\mathrm{CESTR}_2}{1-\mathrm{CESTR}_2} \\ &= \frac{\mathrm{CESTR}_1 + \mathrm{CESTR}_2 - 2 \cdot \mathrm{CESTR}_1 \cdot \mathrm{CESTR}_2}{(1-\mathrm{CESTR}_1) \cdot (1-\mathrm{CESTR}_2)} \end{aligned} \tag{A.3}$$

The factor $\frac{R_{1w}}{k_{sw}}$ was dropped because it is a common factor on both sides of the Eq. (A.3). In addition, when Eq. (A.3) was inverted, we have

$$\begin{aligned} \frac{1}{\mathrm{CESTR}} &= 1 + \frac{(1-\mathrm{CESTR}_1) \cdot (1-\mathrm{CESTR}_2)}{\mathrm{CESTR}_1 + \mathrm{CESTR}_2 - 2 \cdot \mathrm{CESTR}_1 \cdot \mathrm{CESTR}_2} \\ &= \frac{1 - \mathrm{CESTR}_1 \cdot \mathrm{CESTR}_2}{\mathrm{CESTR}_1 + \mathrm{CESTR}_2 - 2 \cdot \mathrm{CESTR}_1 \cdot \mathrm{CESTR}_2} \end{aligned} \tag{A.4}$$

which can be further simplified to be

$$\mathrm{CESTR} = \frac{\mathrm{CESTR}_1 + \mathrm{CESTR}_2 - 2 \cdot \mathrm{CESTR}_1 \cdot \mathrm{CESTR}_2}{1 - \mathrm{CESTR}_1 \cdot \mathrm{CESTR}_2} \tag{A.5}$$

For dilute labile protons undergoing slow and intermediate chemical exchange, the CEST contrast should be small (e.g. a few percent), and it is reasonable to assume that $\mathrm{CESTR}_1 \cdot \mathrm{CESTR}_2 \ll 1$.

Hence, CEST contrast can be shown to be,

$$\begin{aligned} \mathrm{CESTR} \approx\ & (\mathrm{CESTR}_1 + \mathrm{CESTR}_2 - 2 \cdot \mathrm{CESTR}_1 \cdot \mathrm{CESTR}_2) \\ & \times (1 + \mathrm{CESTR}_1 \cdot \mathrm{CESTR}_2 + \mathrm{CESTR}_1^2 \cdot \mathrm{CESTR}_2^2) \approx \mathrm{CESTR}_1 \\ & + \mathrm{CESTR}_2 - \mathrm{CESTR}_1 \cdot \mathrm{CESTR}_2 \cdot (2 - \mathrm{CESTR}_1 - \mathrm{CESTR}_2) \\ & + \mathrm{O}(\mathrm{CESTR}_{1,2}^3) \end{aligned} \tag{A.6}$$

where $\mathrm{O}(\mathrm{CESTR}_{1,2}^3)$ represents the high order coupling term between CEST contrast of multiple labile proton groups, which is often reasonably negligible.

References

[1] S. Forsen, R.A. Hoffman, Study of moderately rapid chemical exchange reactions by means of nuclear magnetic double resonance, J. Chem. Phys. 39 (1963) 2892–2901.

[2] K.M. Ward, A.H. Aletras, R.S. Balaban, A new class of contrast agents for MRI based on proton chemical exchange dependent saturation transfer (CEST), J. Magn. Reson. 143 (2000) 79–87.

[3] K. Snoussi, J.W.M. Bulte, M. Gueron, P.C.M. van Zijl, Sensitive CEST agents based on nucleic acid imino proton exchange: detection of poly(rU) and of a dendrimer-poly(rU) model for nucleic acid delivery and pharmacology, Magn. Reson. Med. 49 (2003) 998–1005.

[4] M. Woods, D.E. Woessner, A.D. Sherry, Paramagnetic lanthanide complexes as PARACEST agents for medical imaging, Chem. Soc. Rev. 35 (2006) 500–511.

[5] J. Zhou, P.C.M. van Zijl, Chemical exchange saturation transfer imaging, Prog. Nucl. Mag. Res. Spectrosc. 48 (2006) 109–136.

[6] S. Aime, D.D. Castelli, S.G. Crich, E. Gianolio, E. Terreno, Pushing the sensitivity envelope of lanthanide-based magnetic resonance imaging (MRI) contrast agents for molecular imaging applications, Acc. Chem. Res. 42 (2009) 822–831.

[7] S. Aime, D. Delli Castelli, F. Fedeli, E. Terreno, A paramagnetic MRI-CEST agent responsive to lactate concentration, J. Am. Chem. Soc. 124 (2002) 9364–9365.

[8] S. Zhang, R. Trokowski, A.D. Sherry, A paramagnetic CEST agent for imaging glucose by MRI, J. Am. Chem. Soc. 125 (2003) 15288–15289.

[9] P.C.M. van Zijl, C.K. Jones, J. Ren, C.R. Malloy, A.D. Sherry, MRI detection of glycogen in vivo by using chemical exchange saturation transfer imaging (glycoCEST), Proc. Natl. Acad. Sci. 104 (2007) 4359–4364.

[10] E. Liepinsh, G. Otting, Proton exchange rates from amino acid side chains-implication for image contrast, Magn. Reson. Med. 35 (1996) 30–42.

[11] S.W. Englander, N.W. Downer, H. Teitelbaum, Hydrogen exchange, Annu. Rev. Biochem. 41 (1972) 903–924.

[12] P.C.M. van Zijl, N. Goffeney, J.H. Duyn, L.H. Bryant, J.W.M. Bulte, The use of starburst dendrimers as pH contrast agents, in: Proc. 9th Annual Meeting ISMRM, Glasgow, 2001, p. 878.

[13] J. Zhou, J. Payen, D.A. Wilson, R.J. Traystman, P.C.M. van Zijl, Using the amide proton signals of intracellular proteins and peptides to detect pH effects in MRI, Nat. Med. 9 (2003) 1085–1090.

[14] P.Z. Sun, J. Zhou, W. Sun, J. Huang, P.C.M. van Zijl, Detection of the ischemic penumbra using pH-weighted MRI, J. Cereb. Blood Flow Metab. 27 (2007) 1129–1136.

[15] P.Z. Sun, P.C.M. van Zijl, J. Zhou, Optimization of the irradiation power in chemical exchange dependent saturation transfer experiments, J. Magn. Reson. 175 (2005) 193–200.

[16] M. McMahon, A. Gilad, J. Zhou, P.Z. Sun, J. Bulte, P.C. van Zijl, Quantifying exchange rates in chemical exchange saturation transfer agents using the saturation time and saturation power dependencies of the magnetization transfer effect on the magnetic resonance imaging signal (QUEST and QUESP): Ph calibration for poly-L-lysine and a starburst dendrimer, Magn. Reson. Med. 55 (2006) 836–847.

[17] P.Z. Sun, C.T. Farrar, A.G. Sorensen, Correction for artifacts induced by B0 and B1 field inhomogeneities in pH-sensitive chemical exchange saturation transfer (CEST) imaging, Magn. Reson. Med. 58 (2007) 1207–1215.

[18] P.Z. Sun, T. Benner, A. Kumar, A.G. Sorensen, An investigation of optimizing and translating ph-sensitive pulsed-chemical exchange saturation transfer (CEST) imaging to a 3 T clinical scanner, Magn. Reson. Med. 60 (2008) 834–841.

[19] P.Z. Sun, Simultaneous determination of labile proton concentration and exchange rate utilizing optimal RF power: radio frequency power (RFP) dependence of chemical exchange saturation transfer (CEST) MRI, J. Magn. Reson. 202 (2010) 155–161.

[20] K.M. Ward, R.S. Balaban, Determination of pH using water protons and chemical exchange dependent saturation transfer (CEST), Magn. Reson. Med. 44 (2000) 799–802.

[21] S. Aime, L. Calabi, L. Biondi, M.D. Miranda, S. Ghelli, L. Paleari, C. Rebaudengo, E. Terreno, Iopamidol: exploring the potential use of a well-established x-ray contrast agent for MRI, Magn. Reson. Med. 53 (2005) 830–834.

[22] J.H. Chen, E.B. Sambol, P. DeCarolis, R. O'Connor, R.C. Geha, Y.V. Wu, S. Singer, High-resolution MAS NMR spectroscopy detection of the spin magnetization exchange by cross-relaxation and chemical exchange in intact cell lines and human tissue specimens, Magn. Reson. Med. 55 (2006) 1246–1256.

[23] R. Avni, O. Mangoubi, R. Bhattacharyya, H. Degani, L. Frydman, Magnetization transfer magic-angle-spinning z-spectroscopy of excised tissues, J. Magn. Reson. 199 (2009) 1–9.

[24] X. Wu, J.J. Listinsky, Effects of transverse cross relaxation on magnetization transfer, J. Magn. Reson. B 105 (1994) 73–76.

[25] J. Pekar, P. Jezzard, D.A. Roberts, J.S. Leigh, J.A. Frank, A.C. Mclaughlin, Perfusion imaging with compensation for asymmetric magnetization transfer effects, Magn. Reson. Med. 35 (1996) 70–79.

[26] S.D. Swanson, Protein mediated magnetic coupling between lactate and water protons, J. Magn. Reson. 135 (1998) 248–255.

[27] A.X. Li, R.H.E. Hudson, J.W. Barrett, C.K. Johns, S.H. Pasternak, R. Bartha, Four-pool modeling of proton exchange processes in biological systems in the presence of MRI-paramagnetic chemical exchange saturation transfer (PARACEST) agents, Magn. Reson. Med. 60 (2008) 1197–1206.

[28] H.M. McConnel, Reaction rates by nuclear magnetic resonance, J. Chem. Phys. 28 (1958) 430–431.

[29] J. Zhou, D.A. Wilson, P.Z. Sun, J.A. Klaus, P.C.M. van Zijl, Quantitative description of proton exchange processes between water and endogenous and exogenous agents for WEX, CEST, and APT experiments, Magn. Reson. Med. 51 (2004) 945–952.

[30] D.E. Woessner, S. Zhang, M.E. Merritt, A.D. Sherry, Numerical solution of the Bloch equations provides insights into the optimum design of PARACEST agents for MRI, Magn. Reson. Med. 53 (2005) 790–799.

[31] P.Z. Sun, J. Zhou, J. Huang, P. van Zijl, Simplified quantitative description of amide proton transfer (APT) imaging during acute ischemia, Magn. Reson. Med. 57 (2007) 405–410.
[32] W. Ling, R.R. Regatte, G. Navon, A. Jerschow, Assessment of glycosaminoglycan concentration in vivo by chemical exchange-dependent saturation transfer (gagCEST), Proc. Natl. Acad. Sci. 105 (2008) 2266–2270.
[33] J. Eng, T.L. Ceckler, R.S. Balaban, Quantitative 1H magnetization transfer imaging in vivo, Magn. Reson. Med. 17 (1991) 304–314.
[34] C.K. Jones, M.J. Schlosser, P.C.M. van Zijl, G.M. Pomper, X. Golay, J. Zhou, Amide proton transfer imaging of human brain tumors at 3 T, Magn. Reson. Med. 56 (2006) 585–592.
[35] J. Hua, C.K. Jones, J. Blakeley, S.A. Smith, P.C.M. van Zijl, J. Zhou, Quantitative description of the asymmetry in magnetization transfer effects around the water resonance in the human brain, Magn. Reson. Med. 58 (2007) 786–793.
[36] R.M. Henkelman, X. Huang, Q.-S. Xiang, G.J. Stanisz, S.D. Swanson, M.J. Bronskill, Quantitative interpretation of magnetization transfer, Magn. Reson. Med. 29 (1993) 759–766.
[37] C. Morrison, R.M. Henkelman, A model for magnetization transfer in tissues, Magn. Reson. Med. 33 (1995) 475–482.